J Mater Sci (2008) 43:3408–3411
DOI 10.1007/s10853-007-2253-y

NANOSMAT 2007 – INTERNATIONAL CONFERENCE ON SURFACES, COATINGS AND NANOSTRUCTURED MATERIALS

Influence of precursor solution coating parameters on structural and dielectric properties of PZT thick films

Byeong-Lib Ahn · Ju Lee · Sang-Man Park · Sung-Gap Lee

Received: 4 July 2007 / Accepted: 23 October 2007 / Published online: 22 February 2008

Abstract Ferroelectric PZT(70/30) thick films were fabricated by the hybrid technique adding the sol-coating process to the normal screen-printing process to obtain a good densification. The screen-printing procedure was repeated four times to form PZT(70/30) thick films, and then PZT(30/70) precursor solution was spin-coated on the PZT thick films. All PZT thick films showed the typical XRD patterns of a perovskite polycrystalline structure. The thickness of all thick films was approximately 75–80 μm. The relative dielectric constant and dielectric loss of the PZT-6 thick film were 656 and 1.2%, respectively. The remanent polarization increased and coercive field decreased with increasing the number of sol coatings and the values of the PZT-6 thick films were 28.3 $\mu C/cm^2$ and 13.1 kV/cm, respectively. Leakage current density of PZT-6 thick films was 2.4×10^{-9} A/cm^2 at 100 kV/cm.

Introduction

In recent years, interest in ferroelectric lead zirconate titanate (PZT) thick films for a wide range of microelectronic and micromechanical applications have increased significantly. Because of its excellent ferroelectric, piezoelectric, and pyroelectric properties, it has been widely used for preparing piezoelectric, ferroelectric, and pyroelectric devices, which include micromachined high-frequency ferroelectric sonar transducers, elastic surface wave devices, new infrared sensors, microelectromechanical system devices, torque sensors, and humidity sensors [1–3]. Especially, the application of thick film technology to ferroelectric ceramics has been performed in a wide range of industrial field because of the simplicity and flexibility of thick film technology. Thick film technologies offer many advantages over the use of bulk ceramics in ferroelectric micro-system devices. Moreover, compared to the thin film technology, the thick film process should allow easier control of both the composition and homogeneity of the complex electronic materials. However, generally the properties of PZT thick films are poorer compared to the bulk ceramics due to their low densification and the lead loss during sintering. To improve properties of thick films, the influences of active powder preparation and of fluxes of sintering were studied. Generally, there is a very large amount of glass frit, such as $Pb_5Ge_3O_{11}$ [4], PbO–Cu_2O [5], and PbO–sPbF_2 [6], which melts during the sintering process, enabling a satisfactory level of densification to be reached. However, these techniques frequently rely on inactive glass frit, which act as low dielectric constant phases in the final film, reducing the dielectric constant, breakdown strength, and other electric properties.

In this study, to obtain a good densification of screen-printed PZT thick films without inorganic glass frit phase, the PZT precursor solution is infiltrated into the screen-printed PZT thick films. And the structural and dielectric properties of the thick films fabricated by the hybrid technique were investigated for application of various transducers and electronic devices.

B.-L. Ahn · J. Lee
Department of Electrical Engineering, Hanyang University, Seoul 133-791, South Korea

S.-M. Park · S.-G. Lee (✉)
Department of Ceramic Engineering, Engineering Research Institute, i-Cube Center, Gyeongsang National University, Gyeongnam 600-701, South Korea
e-mail: lsgap@gnu.ac.kr

Experimental

Ferroelectric $Pb(Zr_{0.7}Ti_{0.3})O_3$ powders were fabricated by a sol–gel method of Pb-acetate trihydrate $[Pb(CH_3CO_2)_2 \cdot 3H_2O]$, Zr *n*-propoxide $[Zr(OCH_2CH_2CH_3)_4]$, and Ti isopropoxide $[\{Ti[OCH(CH_3)_2]_4\}]$, which were dissolved in 2-methoxyethanol ($CH_3OCH_2CH_2OH$). A 10 mol% excess of Pb was added to compensate for the lead loss during heat treatment. The preparation method of the PZT powder was same as that of the previous paper [7]. The screen-printable pastes were prepared by kneading the ground PZT powder with 30 wt.% of organic vehicle (Ferro B75001) in a non-bubbling kneader (NBK-1, Kyoto Electro.). High-purity alumina was used as a substrate. The bottom electrode was prepared by screen printing Pt paste and firing at 1450 °C for 20 min. The PZT pastes were screen-printed on the platinized substrate and were dried at 400 °C for 20 min. The printing and drying procedure was repeated four times. These PZT thick films were sintered at 1050 °C for 2 h in PbO atmosphere. And the $Pb(Zr_{0.3}Ti_{0.7})O_3$ precursor solution was prepared by a sol–gel method and the final concentrations of the solution was 1.0 M. The PZT precursor solution was spin-coated on the PZT thick film using a spinner operated at 2000 rpm for 30 s. These PZT films were dried at 300 °C for 30 min to remove the organic materials. These processes of spin-coating and drying were repeated 0–6 times. These PZT-*n* (*n*: number of sol coatings) thick films, which were spin-coated, precursor solution were annealed at 650 °C for 1 h in the closed alumina crucible.

X-ray diffraction (XRD) was used to determine the crystalline structures of the PZT thick films. This was carried out on a Bruker AXS D8 X-ray diffractometer using CuKα radiation with a step size of 0.01° and a time/step of 5 s. The surface and cross-sectional microstructures were analyzed by a Philips XL30S scanning electron microscopy (SEM). For electrical measurements, the upper electrodes were fabricated by screen-printing Ag paste, and then thick films were poled in a silicone oil bath at 100 °C for 30 min by applying a 35 kV/cm dc field. The electrical properties of the specimens were measured using LCR-meter and ferroelectric test system (Radiant Technologies, RT-66A).

Results and discussions

Figure 1 shows the EDX analysis, which was used for investigating the distribution of surface chemical composition in the thick films. Zr elements decreased and Ti elements increased with increasing the number of spin-coatings because Zr and Ti elements diffused into the adjacent PZT layers. From these results, we inferred that the mixed phases of the rhombohedral PZT(70/30) and the tetragonal PZT(30/70) compositions were formed at each surfaces of PZT grains.

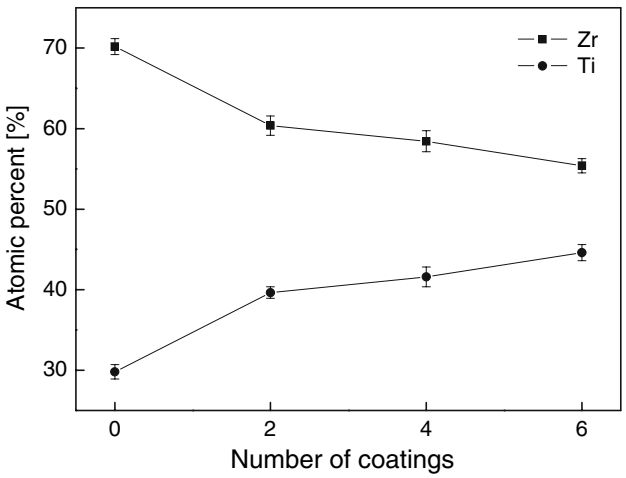

Fig. 1 Surface EDX analysis of the PZT thick films

Figure 2 shows the X-ray diffraction patterns of the PZT thick films printed on Pt/alumina substrate with variation in the number of coatings. All PZT thick films showed the typical XRD patterns of a perovskite polycrystalline structure. The PZT-0 showed the typical XRD pattern of rhombohedral structure. However, the diffraction angle of (112)/(211) plane increased with an increase in the number of coatings and these films showed the XRD patterns characterized by both the tetragonal phase and rhombohedral phase. It can be assumed that the Zr and Ti elements mutually diffused into the adjacent PZT layer.

Figure 3 shows the surface and cross-sectional SEM micrographs of the PZT thick films with the variation in the number of coatings. The PZT-0 thick film was a porous structure and consisted of mixed grains of fine and coarse

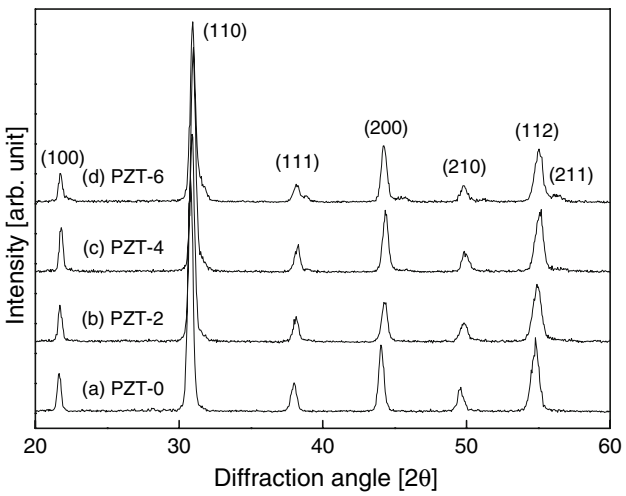

Fig. 2 X-ray diffraction patterns of the PZT thick film with variation in the number of sol coatings

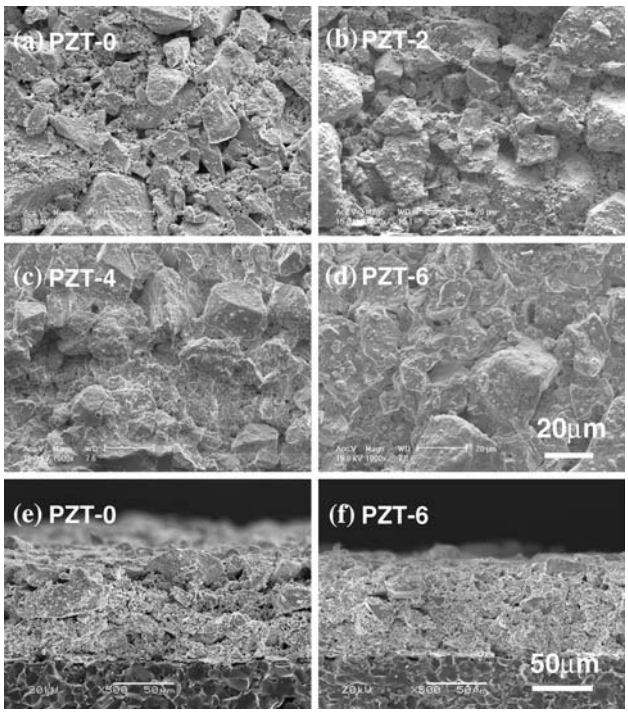

Fig. 3 Surface and cross-sectional SEM micrographs of the PZT thick films with the variation in the number of sol coatings

structure, as shown in Fig. 2a. However, the porosities of surface and inside of films decreased with increasing the number of coatings and the PZT-6 thick films showed good surface flatness and relatively dense cross-sectional microstructure. This result means that the PZT precursor solution was infiltrated between the particles and the agglomeration of particles was promoted with an increase in the number of coatings. The thickness of all thick films was approximately 75–80 μm.

Figure 4 shows the relative dielectric constant and dielectric loss at 1 kHz of PZT thick films with the variation in the number of PZT(30/70) sol coating. The relative

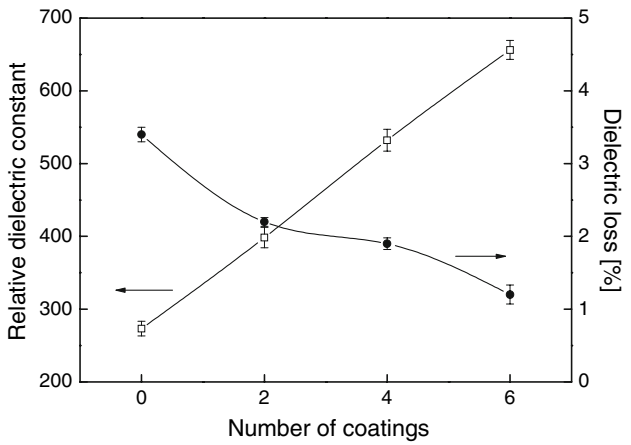

Fig. 4 Relative dielectric constant and dielectric loss at 1 kHz of the PZT thick films with the variation in the number of sol coatings

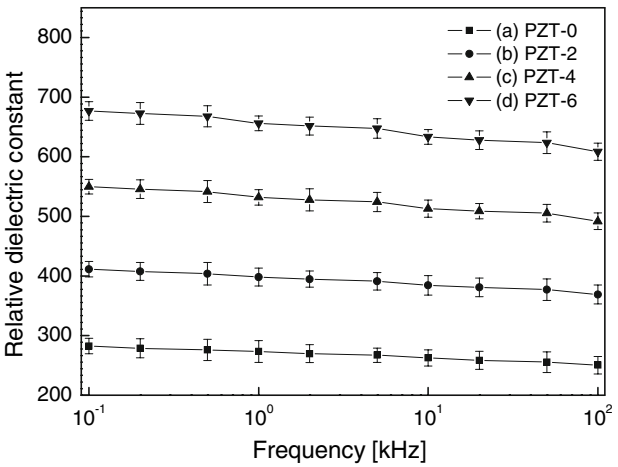

Fig. 5 Relative dielectric constant as a function of the applied frequency

dielectric constant increased and the dielectric loss decreased with increasing the concentration of precursor solutions. The PZT thick films, which were fabricated by the hybrid technique, exhibited a superior dielectric properties compared with the PZT thick film (K = 273) with no sol coating. These properties can be explained by the reduction of porosity and the increment of densification, as shown in the microstructures. The relative dielectric constant and dielectric loss of the PZT-6 thick film were 656 and 1.2%, respectively.

Figure 5 shows the relative dielectric constant as a function of the applied frequency. The relative dielectric constant decreased with increasing the applied frequency and the all PZT thick films showed the typical dielectric dispersion properties [8].

Figure 6 shows the P–E hysteresis loop of the PZT-6 thick films and Fig. 7 shows the remanent polarization and coercive field of PZT thick films with variation in the

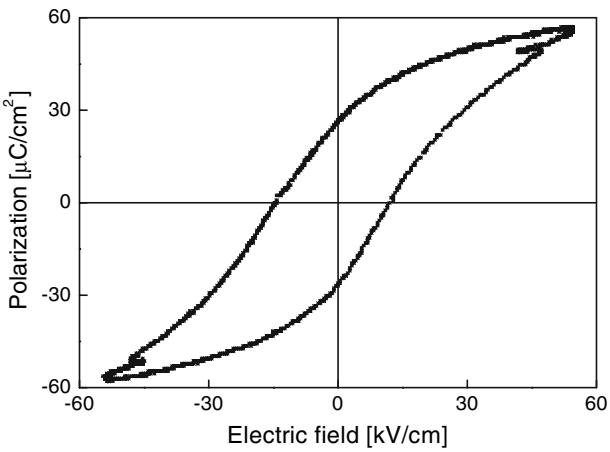

Fig. 6 P–E hysteresis loop of the PZT-6 thick film

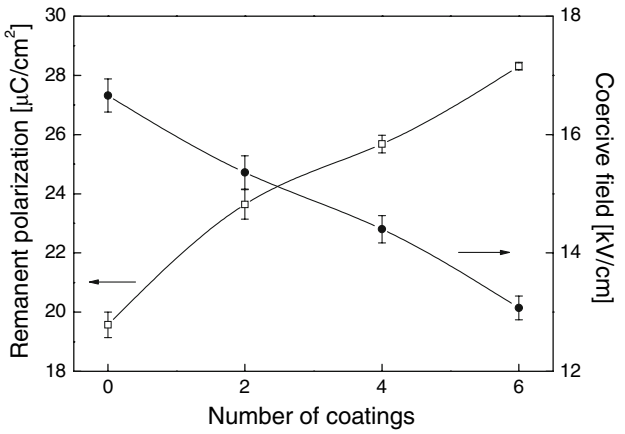

Fig. 7 Remanent polarization and coercive field of PZT thick films with variation in the number of sol coatings

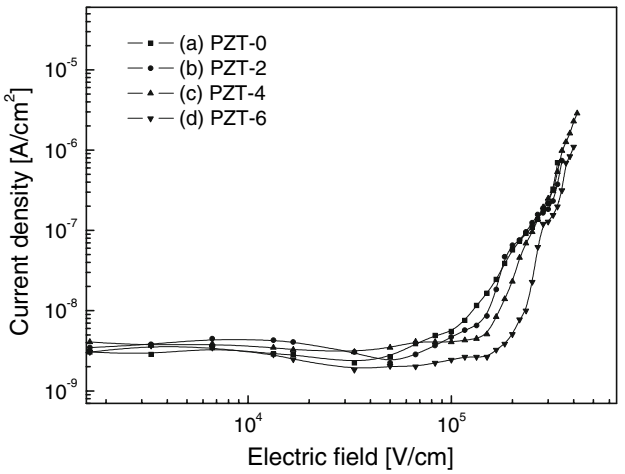

Fig. 8 Current densities of the PZT thick films with the number of sol coatings

number of coatings. The PZT-6 thick film exhibited a relatively well-saturated hysteresis loop. The remanent polarization increased and coercive field decreased with increasing the number of sol coatings. These properties can be understood in terms of the effects of increasing the densification and the coexistence of rhombohedral phase and tetragonal phase or modified PZT phase at the interfaces between PZT(70/30) and PZT(3/70) films such as morphotropic phase boundary region in bulk PZT system [9]. PZT thick films, which were fabricated by the hybrid technique, showed good ferroelectric properties due to the increasine in the polarization efficiency at the interfaces between PZT films.

Figure 8 shows the current densities of the PZT thick films with the number of sol coatings. The leakage current densities slightly decreased with increasing the number of coatings due to the increment of the densification, as shown in Fig. 3. The leakage current densities were less than 10^{-8} A/cm^2 at the applied electric field range of 0–100 kV/cm in all thick films. These values are small enough for their application to various electronic devices. Further investigations and discussions are necessary to understand the leakage current mechanisms in PZT thick films fabricated by the hybrid method.

Conclusions

In this research, ferroelectric PZT(70/30) thick films were fabricated by the hybrid technique adding the sol-coating process to the normal screen-printing process. Structural and dielectric properties were investigated with variation in the number of sol coatings. PZT thick films showed the XRD patterns characterized by both the tetragonal phase and rhombohedral phase because the Zr and Ti elements mutually diffused into the adjacent PZT layer. The densification of the thick films was increased with increasing the number of coatings. The thickness of all thick films was approximately 75–80 μm. The dielectric properties such as relative dielectric constant, remanent polarization, and leakage current density of PZT-6 thick films were superior to those of PZT-0 thick films with no sol coating, and those values for the PZT-6 film were 656, 28.3 μC/cm^2, and 2.4×10^{-9} A/cm^2 at 100 kV/cm, respectively.

Acknowledgement This work has been supported by KESRI (R-2005-7-094), which is funded by MOCIE (Ministry of Commerce, Industry and Energy).

References

1. Scott JF, Araujo CA (1989) Science 246:1400
2. Newnham RE, Ruschanu GR (1991) J Am Ceram Soc 74:463
3. Whatmore RW, Osbond PL, Shorrocks NM (1987) Ferroelectrics 76:351
4. Watton R, Smith C, Jones GR (1976) Ferroelectrics 14:719
5. Corker DL, Zhang Q, Whatmore RW, Perrin C (2002) J Eur Ceram Soc 22:383
6. Tanaka K, Kubota T, Sakabe Y (2002) Sens Actuators 96:179
7. Lee SG, Kim CJ (2006) J Kor Phys Soc 49:216
8. Buchanan RC (1986) Ceramic materials for electronics. Dekker, New York, p 47
9. Lee SG, Kim KT, Lee YH (2000) Thin Solid Films 372:45